

Seismic Strengthening of Boundary Columns in R/C Shear Walls

Y. Sanada

Osaka University, Japan

H. Takahashi & H. Toyama

Toyohashi University of Technology, Japan



SUMMARY:

This paper proposes and describes a new method for seismically strengthening vulnerable existing reinforced concrete shear walls, which do not satisfy current Japanese structural provisions. The proposed method improves the seismic performance of shear walls by confining only boundary columns using steel shapes and high-strength steel rods. A series of structural tests was conducted using four shear wall specimens: two normal specimens with different failure modes and two strengthened specimens applying the proposed method to normal specimens. As a result, the unstrengthened specimens failed in a brittle manner and lost their axial resistance after shear failure. Large compressive deformations after shear failures of unstrengthened specimens were caused by slip behaviour along diagonal shear cracks, which was modelled by a simple trigonometric equation. On the other hand, the strengthened specimens exhibited stable behaviour, and confining the boundary columns successfully prevented shear failure.

Keywords: Existing building, reinforced concrete, retrofit

1. INTRODUCTION

A large number of seismic strengthening methods have been proposed for existing reinforced concrete (R/C) buildings. Most of them were developed for application to columns, whereas several seismic strengthening methods for shear walls have been presented in previous studies. For instance, Takara et al. (2008) proposed two retrofit techniques that confined shear walls with concrete, steel plates, and high-strength tensioning rods. Kim et al. (2012) applied flexible polyester fibre sheets to upgrade the seismic performance of shear walls. However, such studies focused mainly on regular shear walls, and the methods presented might occasionally have difficulties in practical application: e.g. structural complexities can be found when openings and/or perpendicular walls are planned inside/beside shear walls.

In this study, an alternative method of seismic strengthening is proposed for vulnerable existing R/C shear walls, which do not satisfy current Japanese structural provisions (AIJ 2010). The proposed method improves the seismic performance of shear walls by partially confining only boundary columns using steel shapes and high-strength steel rods. It can be applied in the same manner not only to regular shear walls but also to irregular ones with openings and/or perpendicular walls, because strengthening materials are attached only to two surfaces (exterior and interior surfaces) of each boundary column.

This paper describes a series of structural tests investigating the seismic performance of typical existing R/C shear walls in Japan with/without the proposed strengthening method. An example of potential progressive collapse due to a vulnerable failure of unstrengthened shear wall is also introduced.

2. STRENGTHENING METHOD

This study proposes a new method for seismically strengthening vulnerable existing R/C shear walls. The proposed method improves the seismic performance of shear walls by partially confining only boundary columns using steel shapes and high-strength steel rods. Figure 1 illustrates the retrofit scheme. The application procedure, which is illustrated with the shear wall specimen described below, is as follows:

Step 1: A C-shaped steel channel and L-shaped steel angles are attached to the exterior and interior surfaces of boundary column, respectively, as shown in Fig. 1. A slit of 10 mm is designed at the top of each steel shape, which is not subjected a direct compression from a beam above. Mortar is applied between the boundary column and channel/angles.

Step 2: High-strength steel rods are inserted penetrating the column and steel shapes, as shown in Fig. 2. The diameter of a steel rod is 7.1 mm.

Step 3: After achieving the expected mortar strength, the steel rods are tensioned with a strain of 500μ .

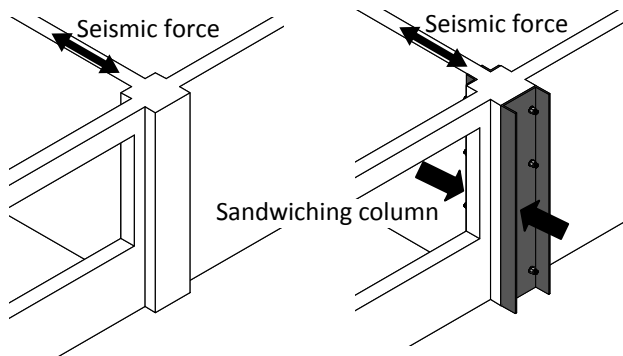


Figure 1. Retrofit scheme

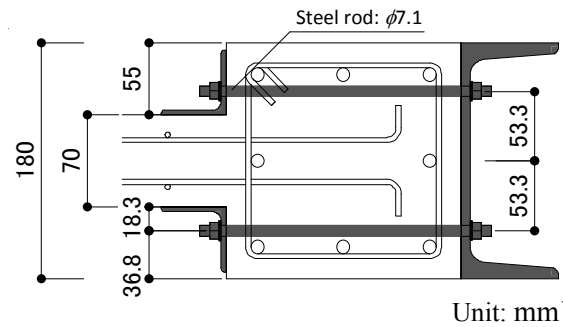


Figure 2. Cross-section of boundary column

3. EXPERIMENTAL PROGRAM

3.1. Test Specimens

Four 3/10 scale specimens were prepared representing typical existing R/C shear walls in Japan, which do not satisfy the current Japanese structural provisions (AIJ 2010). All specimens had the same structural details, as shown in Fig. 3 and Table 1, whereas two types of failure mechanism were

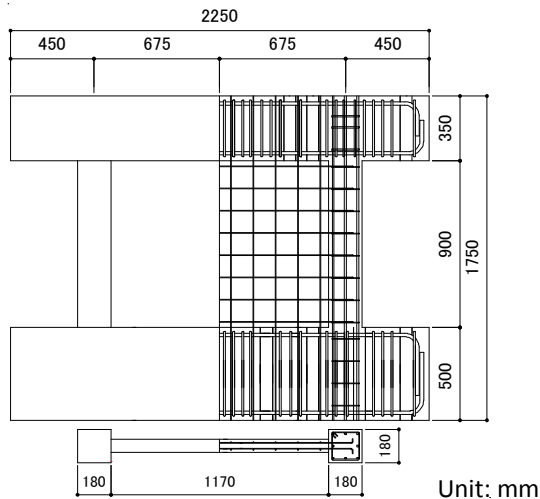


Figure 3. Details of unstrengthened specimens

Table 1. Details of unstrengthened specimens

Column	Cross-section	180×180 mm
	Main bar	8-D10
	Stirrup	D4@120
	p_w	0.13%
Wall	Thickness	70mm
	Reinforcement	D4@double ($p_s=0.31\%$)

where, p_w : shear reinforcement ratio, p_s : ratio of horizontal/vertical reinforcement.

planned by controlling shear span-depth ratio under lateral loads. SW0.8 and SW0.4 were unstrengthened specimens designed to fail in bending and shear, respectively. However, the numbers in the names of specimens represent the shear span-depth ratio, which is explained in detail at Section 3.3. The proposed seismic strengthening method was applied to two of the specimens: RW0.8 and RW0.4, which are described in detail in Section 6. Material properties of rebars and concrete are listed in Table 2.

Table 2. Material properties

Concrete	E_c	σ_B	σ_t	Rebar	Diameter	E_s	f_y	ϵ_y
	N/mm ²	N/mm ²	N/mm ²			N/mm ²	N/mm ²	μ
	2.55×10^4	27.6	2.65		D4	1.47×10^5	349	4282
			D10	1.93×10^5	370	1949		

where, E_c, E_s : Young's modulus, σ_B : compressive strength, σ_t : tensile strength, f_y : yield stress, ϵ_y : yield strain.

3.2. Measurements

Figure 4 shows the transducers set-up to measure the horizontal, vertical and diagonal relative displacements of specimens. D1 in the figure is a transducer that measures the horizontal relative displacement used for controlling lateral loads. Strains of reinforcements were measured using several strain gauges adhered to longitudinal and shear reinforcements in the boundary columns and wall panel. Moreover, at the peak and residual drifts in each loading cycle described below, initiated cracks, crack propagation, and crack widths measured by visual inspection were marked on the specimens to identify the failure mechanisms of specimens.

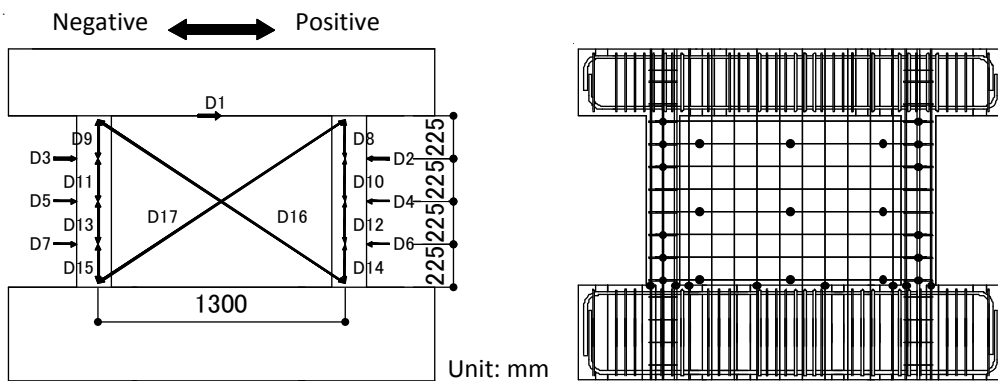


Figure 4. Arrangements of displacement transducers and strain gauges

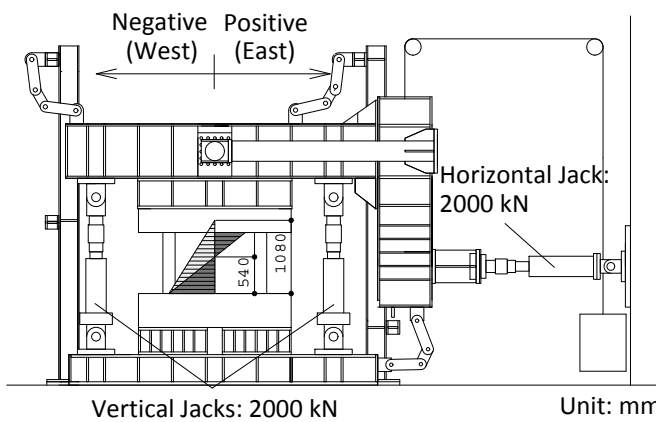


Figure 5. Schematic view of test set-up

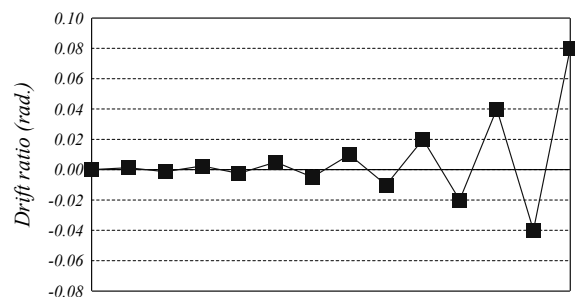


Figure 6. Loading history in the horizontal direction

3.3. Loading Method

A schematic representation of the experimental set-up is shown in Fig. 5. Each specimen was fixed at its upper and lower stubs to the loading frames. Reversed cyclic lateral loads were applied to the specimens under a constant axial load of 300 kN. Shear span-to-depth ratios of 0.8 and 0.4 were maintained by controlling vertical jacks for SW0.8 and RW0.8, and SW0.4 and RW0.4, respectively. Incremental lateral loads were controlled by top drift ratio, R , which was measured with the transducer D1 in Fig. 4. The lateral loading program had an initial cycle to $R=1/800$, followed by two cycles to $R=1/400$, $1/200$, $1/100$, $1/50$, and $1/25$, and a pushover to $R=1/12.5$, as shown in Fig. 6.

4. TEST RESULTS FOR UNSTRENGTHENED SPECIMENS

4.1. Failure Process

4.1.1. SW0.8

Initial flexural and shear cracks were observed at the bottom of the boundary column and the wall panel, respectively, in the first cycle to $R=1/800$. Initial shear cracks at the ends of columns occurred in the following cycle to $R=1/400$. The specimen began to yield in bending during the cycle to $R=1/200$, where longitudinal rebars in the column and wall initially yielded. Spalling of concrete cover was observed on the wall panel in the cycle to $R=1/100$. The specimen failed in shear during the first cycle to $R=1/50$, then it completely lost the axial resistance during the second cycle. Figure 7a shows the damage to the specimen after the test.

4.1.2. SW0.4

Similar behaviour to SW0.8 was observed until the cycle to $R=1/400$. In this specimen, however, significant shear cracks occurred at the top of the tensile column and developed diagonally to the bottom of the compressive column during the cycle to $R=1/200$. As a result, the lateral strength rapidly deteriorated during this cycle. Diagonal cracks developed as shown in Fig. 7b.



Figure 7. Damage to unstrengthened specimens after testing

4.2. Lateral Force-Drift Ratio Relationship

4.2.1. SW0.8

Figure 8a shows the lateral force-drift ratio relationship of SW0.8. Stiffness was initially degraded with initial flexural and shear cracks at the tensile column and wall, respectively. The maximum lateral strength of 554 kN was recorded during the cycle to $R=1/100$, which exceeded the theoretical flexural strength. Then, the lateral resistance dropped rapidly to about 20% of the maximum strength after shear failure around $R=1/100$ during the cycle to $R=1/50$. It also lost axial resistance during this cycle.

4.2.2. SW0.4

The specimen exhibited similar behaviour to SW0.8 at small drift levels. As shown in Fig. 8b, however, it failed in shear prior to flexural yielding. The maximum lateral strength was 630 kN which was recorded during the cycle to $R=1/200$. Then, the lateral drift jumped to $R=1/100$ with rapid strength deterioration, and the shear resistance dropped to about 50% of the maximum strength. The specimen completely lost its horizontal and axial load carrying capacities during the cycle to $R=1/50$.

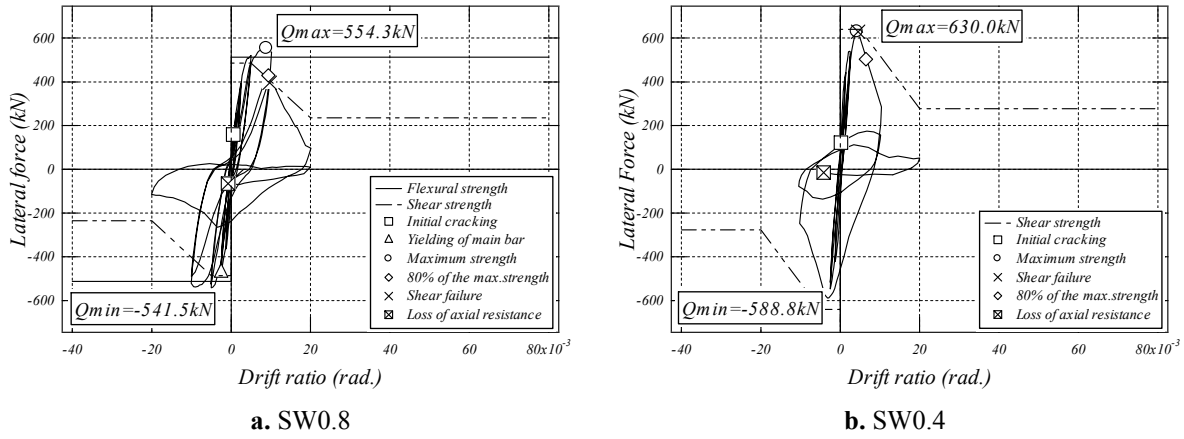


Figure 8. Lateral force-drift ratio relationships

4.3. Post-Peak Behaviour

Figure 9 shows the axial deformation-lateral drift ratio relationships of both specimens, which indicate that compressive deformations increased significantly after the specimens failed in shear. Sliding behaviour was also observed along the diagonal shear cracks, which are shown in Fig. 7, after the shear failure. Therefore, the relationship between axial deformation and lateral drift seems to be represented by a simple trigonometric equation (Eq. 1), as illustrated in Fig. 10.

$$\delta_y = \delta_x \cdot \tan \theta \quad (1)$$

where, δ_y , δ_x , θ : refer to Fig. 10.

Figure 11 shows the relationships between cumulative axial deformation and cumulative lateral drift for both specimens. However, the cumulative axial deformation of each column was obtained with a coordinate relative to the point of shear failure in each loading direction, as explained in Fig. 12. Comparing with the calculation by Eq. 1, it was found that the inclinations obtained with Eq. 1 agreed well with the experimental results in the ultimate state.

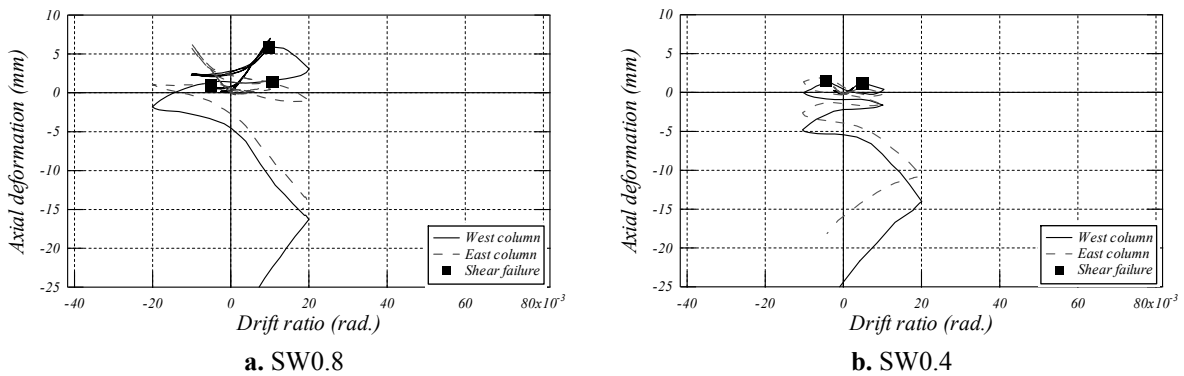


Figure 9. Axial deformation-lateral drift ratio relationships

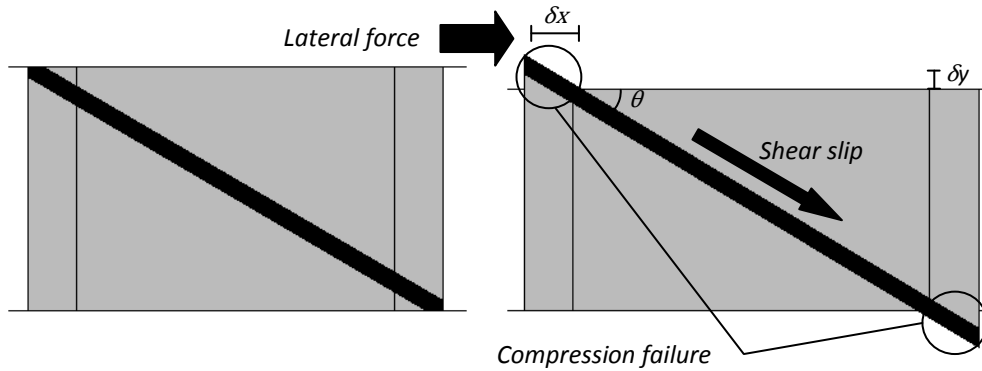


Figure 10. Shear slip behaviour

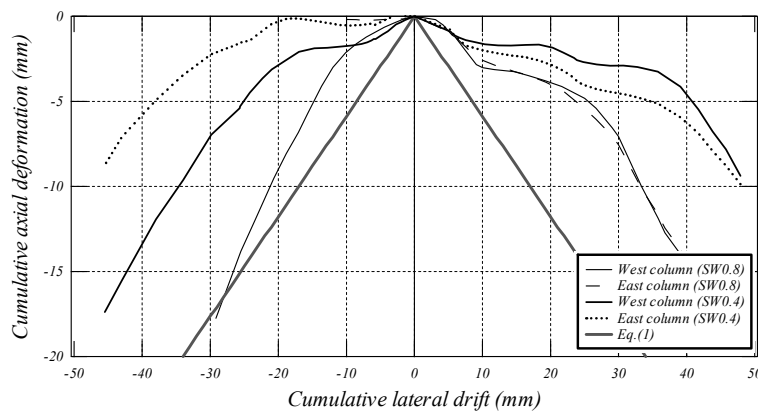


Figure 11. Cumulative axial deformation-cumulative lateral drift relationships after shear failure

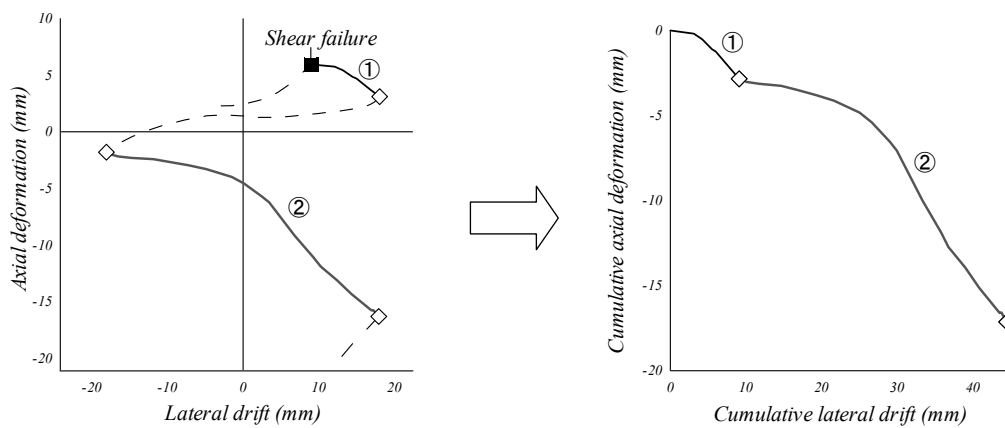


Figure 12. How to draw Fig. 11

5. INVESTIGATION ON POTENTIAL RISK OF PROGRESSIVE COLLAPSE

5.1. Analytical Structure

The structure analyzed was a single-story frame partially extracted from a typical four-story R/C school building in Japan (JBDPA 2005), as shown in Fig. 13. Figure 14 shows the modelling of the structure. In the following analysis, however, responses of the structure were evaluated only along the X axis in Fig. 13.

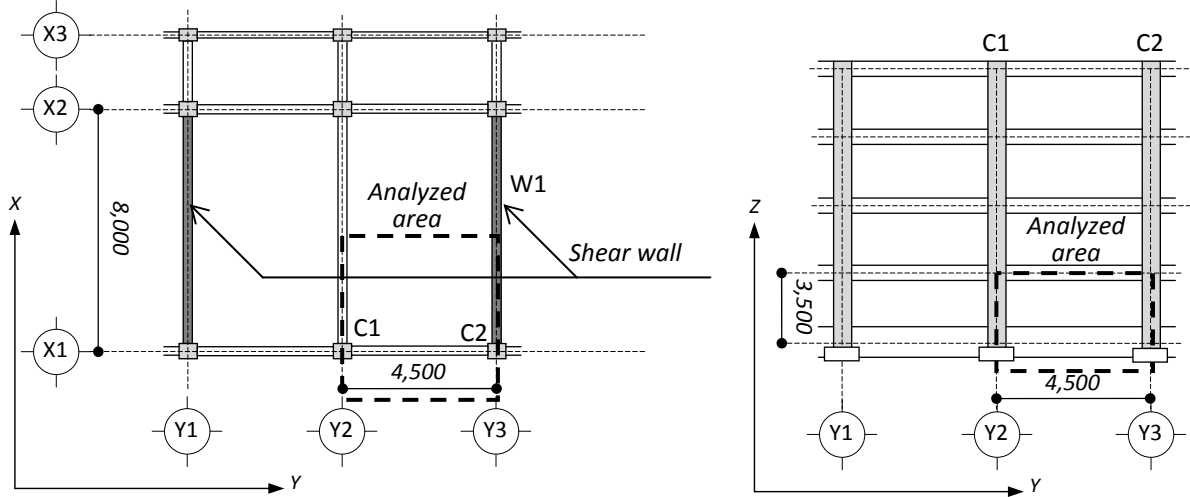


Figure 13. Analytical structure

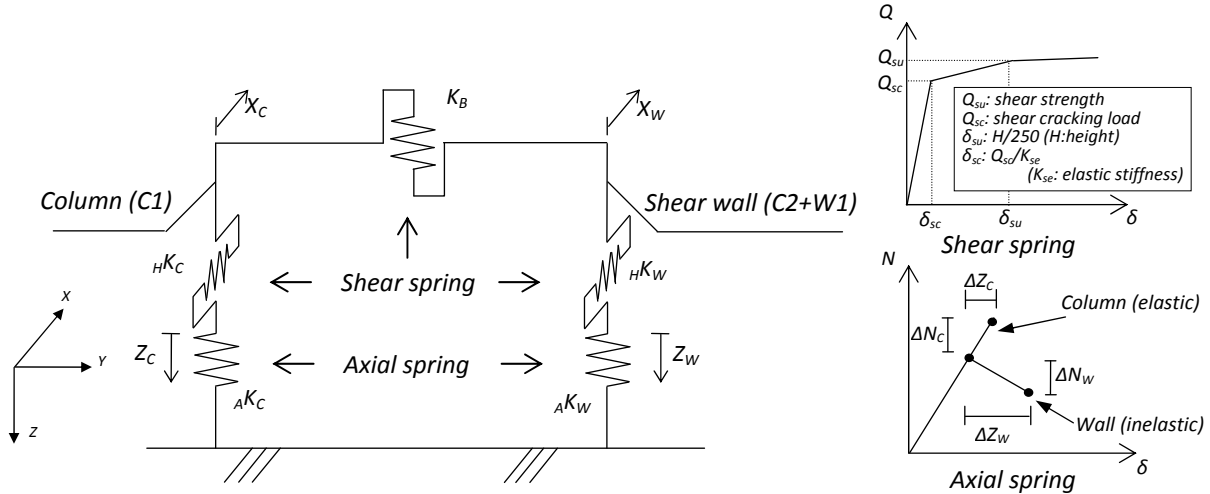


Figure 14. Modelling

5.2. Analytical Method Considering the Post-peak Behaviour of Shear Walls

In this analysis, the post-peak behaviour of shear walls, which is the compressive deformation after shear failure represented by Eq. 1, was considered as follows:

- 1) An incremental axial deformation of shear wall is evaluated with Eq. 2 (Eq. 1).

$$\Delta Z_W = \Delta X_W \cdot \tan \theta \quad (2)$$

where, ΔZ_W : incremental axial deformation of shear wall, ΔX_W : incremental lateral drift of shear wall (refer to Fig. 14).

- 2) Incremental axial forces of column and shear wall, which are transferred by the beam with axial deformation of shear wall, are obtained with Eqs. 3 and 4.

$$\Delta N_C = K_B \cdot (\Delta Z_W - \Delta Z_C) \quad (3)$$

$$\Delta N_W = K_B \cdot (\Delta Z_C - \Delta Z_W) \quad (4)$$

where, ΔN_C : incremental axial force of column, ΔN_W : incremental axial force of shear wall, K_B : shear stiffness of beam, ΔZ_C : incremental axial deformation of column (refer to Fig. 14).

3) The incremental axial deformation of column can be evaluated with Eq. 5 from Eqs. 3 and 6.

$$\Delta Z_C = \frac{K_B \cdot \Delta Z_W}{{}_A K_C + K_B} \quad (5)$$

$$\Delta N_C = {}_A K_C \cdot \Delta Z_C \quad (6)$$

where, ${}_A K_C$: axial stiffness of column (refer to Fig. 14).

4) The axial stiffness of shear wall is finally determined with Eq. (7) from Eqs. (4) and (8).

$${}_A K_W = \frac{K_B \cdot (\Delta Z_C - \Delta Z_W)}{\Delta Z_W} \quad (7)$$

$$\Delta N_W = {}_A K_W \cdot \Delta Z_W \quad (8)$$

where, ${}_A K_W$: axial stiffness of shear wall (refer to Fig. 14).

5.3. Analytical Results

The 1995 JMA Kobe acceleration record (NS) was used for the earthquake response analysis. Damping was assumed to be proportional to initial stiffness with a damping ratio of 5%. Figure 15 shows the time histories of lateral drifts, axial deformations and axial forces of column and wall. The shear wall failed in shear at about 4 sec. from Fig. 15a, then exhibited large compressive deformation from Fig. 15b. As a result, the column adjacent to shear wall carried a larger axial load, which was 2.7 times before the shear failure of the wall. This result indicates the potential risk of a progressive collapse of this kind of structure.

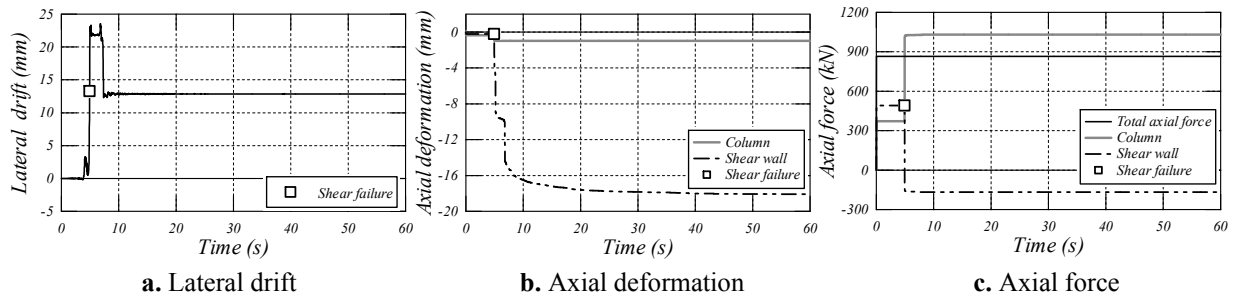


Figure 15. Analytical results

6. VERIFICATION OF STRENGTHENING

6.1. Summary of Verification

The strengthening method proposed in Section 2 was applied to two of the specimens described in Section 3.1. Figure 16 illustrates details of strengthened specimens and steel shapes used for strengthening. Yield stresses of strengthening materials were 1092 N/mm^2 and 332 N/mm^2 for high-strength steel rods of $\phi 7$ and steel shapes, respectively. The tests were conducted in the same manner as described in Sections 3.2 and 3.3. Experimental results are compared between unstrengthened and strengthened specimens in the following.

6.2. Comparisons of Test Results

6.2.1. Failure process

Compared to the unstrengthened specimens, RW0.8 and RW0.4 behaved in similar manners until the

cycles to $R=1/100$ and $R=1/400$, respectively. Then, in the cases of strengthened specimens, concrete crushing occurred particularly between the column and wall during the cycles to $1/50$ and $1/200$ for SW0.8 and SW0.4, respectively. Shear failure occurred only at the wall panels in the cycles to $1/50$ and $1/100$ for SW0.8 and SW0.4, whereas the boundary columns avoided shear failure at the ends. Therefore, they could still support the axial loads. Figure 17 shows the damage to strengthened specimens after the tests.

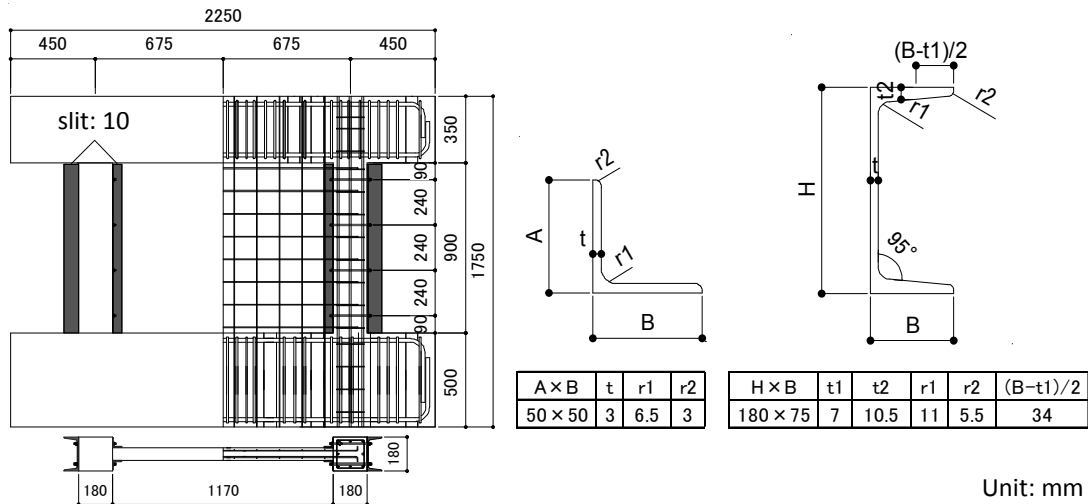
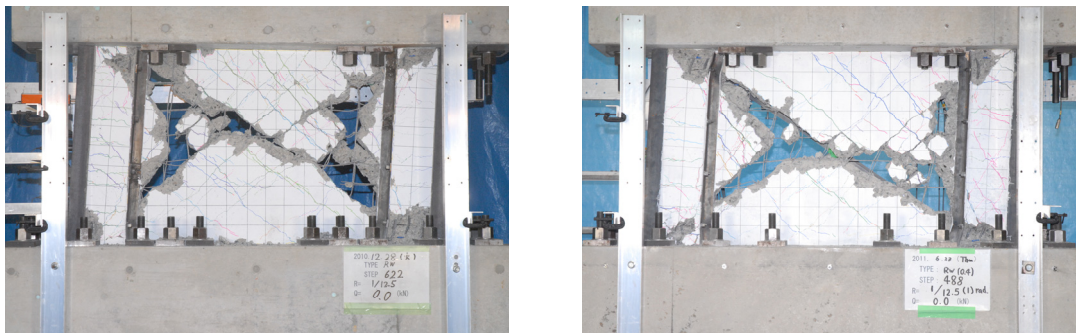


Figure 16. Details of strengthened specimens



a. RW0.8

b. RW0.4

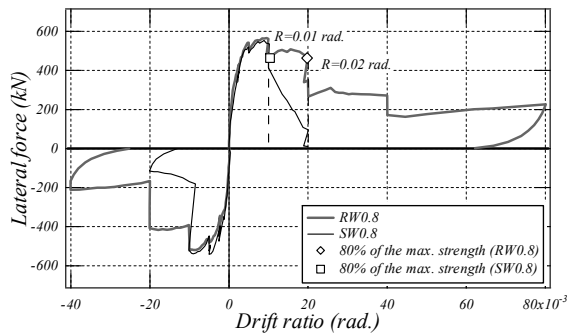
Figure 17. Damage to strengthened specimens after testing

6.2.2. Lateral force-drift ratio relationship

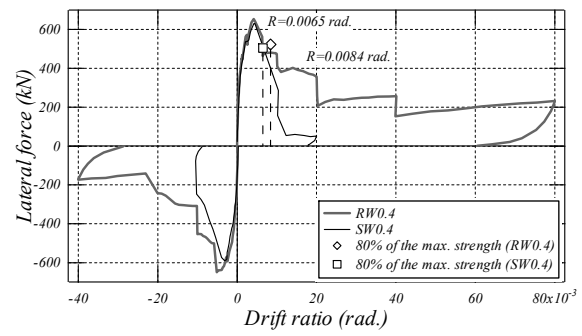
Figure 18 compares the envelope curves of lateral force-drift ratio relationships between the strengthened and unstrengthened specimens. Strengthened specimens exhibited similar envelope curves until the unstrengthened specimens failed in shear. Although neither of the strengthened specimens significantly exceeded the maximum strengths of unstrengthened specimens (even in the case of shear-critical wall, RW0.4), the deformation capacities, which were obtained at 80% of the maximum strengths, were improved by about 100% and 30% for RW0.8 and RW0.4, respectively. Horizontal strengths were not completely lost throughout the tests because the columns did not lose their axial load-carrying capacities.

6.2.3. Post-peak behaviour

In the cases of strengthened specimens, the columns did not lose their axial resistances, which differed from the test results for unstrengthened specimens. The columns were finally separated from the wall panel with severe damage to concrete at the boundaries, as shown in Fig. 17. They behaved like an independent column in the ultimate state. Consequently, the columns were prevented from suffering shear and axial failure, as shown in Fig. 19, because they were not subjected to high punching shear forces from the wall panels.

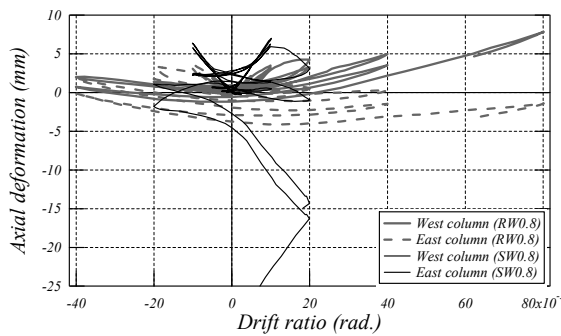


a. RW0.8 and SW0.8

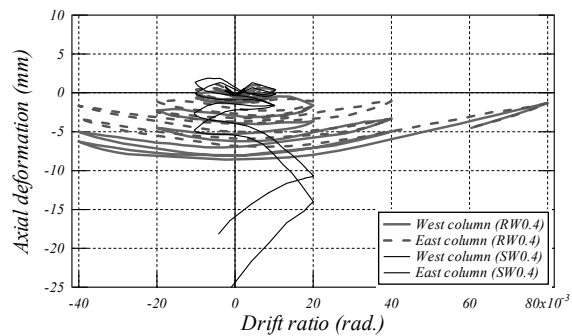


b. RW0.4 and SW0.4

Figure 18. Comparisons between lateral force-drift ratio relationships



a. RW0.8 and SW0.8



b. RW0.4 and SW0.4

Figure 19. Comparisons between axial deformation-lateral drift ratio relationships

7. CONCLUSIONS

A new strengthening method is proposed for existing R/C shear walls that do not satisfy current Japanese structural provisions. Four shear wall specimens were prepared and tested to clarify the contribution of strengthening to seismic performance. Major conclusions are summarized as follows:

- 1) Applying the strengthening method to flexure-dominant and shear-critical walls, deformation capacities were improved by 100% and 30%, respectively.
- 2) The strengthening method prevented RW0.8 and RW0.4 from suffering axial failure as well as shear failure. Consequently, horizontal resistances were not completely lost, and axial load-carrying capacities were maintained.
- 3) On the other hand, in the cases of SW0.8 and SW0.4, shear failure finally occurred. The column ends were damaged significantly by shear slip behaviour, which might cause progressive collapses of old and vulnerable R/C buildings in Japan.

REFERENCES

- Architectural Institute of Japan (AIJ). (2010). AIJ Standard for Structural Calculation of Reinforced Concrete Structures (in Japanese).
- The Japan Building Disaster Prevention Association (JBDPA). (2005). English Version 1st, Standard for Seismic Evaluation of Existing Reinforced Concrete Buildings, 2001.
- Kim, Y., Kabeyasawa, T. and Igarashi, S. (2012). Dynamic collapse test on eccentric reinforced concrete structures with and without seismic retrofit. *Engineering Structures* **34**, 95-110.
- Takara, S., Yamakawa, T. and Yamashiro, K. (2008). Experimental and Analytical Investigation of Seismic Retrofit for RC Framed Shear Walls. *The 14th World Conference on Earthquake Engineering*. 12-01-0031.